Real-Time Parameter Estimation of DC–DC Converters Using a Self-Tuned Kalman Filter

Mohamed Ahmeid, Matthew Armstrong, Shady Gadoue, Maher Al-Greer, and Petros Missailidis

***Abstract*—To achieve high-performance control of modern dc–dc converters, using direct digital design techniques, an accurate discrete model of the converter is necessary. In this paper, a new parametric system identification method, based on a Kalman filter (KF) approach is introduced to estimate the discrete model of a synchronous dc–dc buck converter. To improve the tracking performance of the proposed KF, an adaptive tuning technique is proposed. Unlike many other published schemes, this approach offers the unique advantage of updating the parameter vector coefficients at different rates. The proposed KF estimation technique is experimentally verified using a Texas Instruments TMS320F28335 microcontroller platform and synchronous step-down dc–dc converter. Results demonstrate a robust and reliable real-time estimator. The proposed method can accurately identify the discrete coefficients of the dc–dc converter. This paper also validates the performance of the identification algorithm with time-varying parameters, such as an abrupt load change. The proposed method demonstrates robust estimation with and without an excitation signal, which makes it very well suited for real-time power electronic control applications. Furthermore, the estimator convergence time is significantly shorter compared to many other schemes, such as the classical exponentially weighted recursive least-squares method.**

***Index Terms*—DC–DC converter, Kalman filter (KF), parameter estimation, recursive least-squares (RLS) method, system identification.**

I. Introduction

SWITCH-MODE dc–dc power converters are widely used in a variety of applications, ranging from dc motor drives, personal computers, home appliances, and portable electronic devices [1], [2]. All of these applications require efficient and cost-effective dynamic and steady-state voltage or power regulation over a wide range of operating conditions. Traditionally, predesigned PID controllers are applied to achieve the required dynamic performance in these systems. However, poor knowledge of the power converter parameters may cause inaccuracies in the controller design. Moreover, unpredicted behaviors such as sudden load variations, components aging, noise, and unpredictable changes in operating mode may degrade the controller performance and can lead to instability within the entire system [3], [4]. For these reasons, adaptive and autotuning controllers, based on the system identification of the converter parameters, are now gaining more attention.

Recently, several techniques for the system identification of dc–dc converters have been proposed. Two main classes of system identification are commonly employed: parametric and nonparametric techniques. In nonparametric identification methods, the system frequency response is determined directly, with no prior knowledge of the system model [5], [6]. The proposed strategies include correlation analysis [7], [8], transient response analysis [9], [10], Fourier, and spectral analysis [11], [12]. Typically, nonparametric system identification approaches assume steady-state operation and the system identification process is carried out, while the control loop is open to inject the excitation signal. In addition, the frequency response measurements are usually performed offline on a host PC or a field-programmable gate array, which increases the complexity and hence the cost of the implementation [6]. Also, by incorporating these techniques in real-time applications such as dc–dc power converters, abrupt changes in the parameters can potentially yield unpredicted behavior or even an unstable output response. The second paradigm, parametric system identification, assumes a known model structure with prespecified order and number of coefficients to be estimated [5]. According to the literature, conventional least squares [5], [13] and its recursive version, recursive least squares (RLS) [4], [14], [15], are the most commonly used algorithms for parameter estimation of dc–dc converters. In [4], the classical RLS algorithm is reviewed and tested in real time on an open-loop buck converter. It is confirmed that the classical RLS algorithm can result in accurate parameter estimation for systems with fixed, or slow varying, loads while operating at sampling frequency much lower than the switching frequency. However, the algorithm fails to track fast parameter changes. In order to overcome this problem, the exponentially weighted RLS (ERLS) algorithm is often applied to estimate abrupt changes in converter parameters. An offline parameter estimation approach is presented in [14] using the biogeography-based optimization method. Due to the low sampling rate used in this approach, the estimation process takes around 100 ms to converge to its final values. In addition, the proposed method has a considerably higher computational cost compared to ERLS. A low computational complexity ERLS identification technique, based on a dichotomous coordinate

Manuscript received March 31, 2016; revised July 13, 2016; accepted August 22, 2016. Date of publication September 7, 2016; date of current version February 27, 2017. Recommended for publication by Associate Editor M. Ordonez.

M. Ahmeid, M. Armstrong, M. Algreer, and P. Missailidis are with the School of Electrical and Electronic Engineering, Newcastle University, Newcastle Upon Tyne, NE1 7RU, U.K. (e-mails: mohamed.ahmeid@ncl.ac.uk; matthew.armstrong@ncl.ac.uk; maher.al-greer@ncl.ac.uk; petros.missailidis@ncl.ac.uk).

S. Gadoue is with the School of Electrical and Electronic Engineering, Newcastle University, Newcastle upon Tyne, NE1 7RU, U.K., and also with the Department of Electrical Engineering, Faculty of Engineering, Alexandria University, Alexandria 21544, Egypt (e-mail: shady.gadoue@ncl.ac.uk).

Color versions of one or more of the figures in this paper are available online at http://ieeexplore.ieee.org

Digital Object Identifier 10.1109/TPEL.2016.2606417

descent algorithm, is introduced in [2]. However, according to simulation and initial experimental results, the proposed method is tested offline showing a slow convergence time for zero coefficients with modest fluctuation due to measurement noise. In addition, the performance of the proposed algorithm is not investigated during abrupt load changes. Regardless of the improvement introduced by ERLS in terms of estimating abrupt changes, it is reported that a compromise must be made between noise sensitivity and dynamic tracking performance [15]. Typically, this technique applies equal weight to all parameters during the estimation process. As a result, if the rate of variation of one of the estimated parameters is greater than the other parameters, the same adaptation gain correction is applied to all parameters irrespectively which greatly affects the estimator output [16]. The estimation of coefficients with small values will suffer from slow convergence speed and higher estimation error. Practically, the measurement noise may increase this deviation, which impacts on the reliability of the estimation results when used in fault detection applications or controller design on the fly. This scenario is illustrated in parameter estimation of dc–dc converters, where sluggish convergence of the zero coefficients is observed and their final value is highly affected by the measurement noise [2]. Another drawback of the ERLS implementation is the requirement of superimposing the input signal with a frequency-rich signal [such as those generated by a pseudorandom binary sequence (PRBS)] to enhance the estimation accuracy and prevent estimator wind up due to an exponential growth of the adaptation gain matrix [16]. This necessitates keeping the output voltage perturbed for long periods or resetting the estimator periodically, which can lead to some abrupt changes not being observed. To overcome this, the error covariance matrix can be updated using a different approach to add more freedom to the adaptive algorithm when calculating the adaption gain. In this paper, a state-of-the-art Kalman filter (KF) algorithm is proposed for real-time parameter estimation of a switch-mode power converter (SMPC). The proposed technique has the advantage of providing an independent strategy for adaptation of each individual parameter. Compared to existing system identification approaches, the proposed algorithm can be readily implemented online and is well suited for real-time dynamic applications. Furthermore, unlike classical RLS approaches, the effects of the excitation signal and parameter uncertainty can be factored into the proposed algorithm. This results in greater precision parameter estimation and much faster convergence speed. The effectiveness of the proposed technique is experimentally verified on a synchronous buck converter operating in continuous conduction mode (CCM); however, it can be easily transferred to other converter topologies. Results also confirm the ability of the proposed KF algorithm to produce improved performance compared to commonly applied ERLS schemes.

II. Parameter Estimation of SMPC

A. Discrete Time Modeling

Generally, in parametric paradigms, the candidate model of the unknown system should be known in advance. In this research, a synchronous dc–dc buck converter is considered

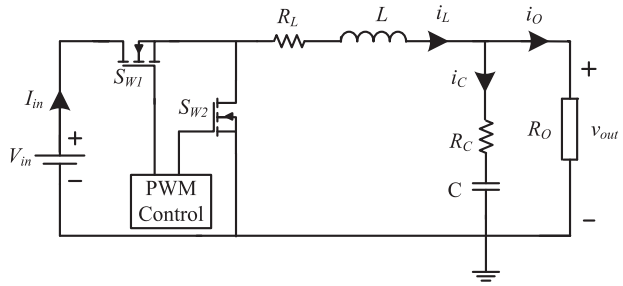

Fig. 1. Synchronous buck converter.

(see Fig. 1). The analytical model of this converter is well understood and defined in the literature [2], [14]; consequently, the validated result will be used directly in this paper. Furthermore, the derivation of the average model for the buck converter is well reported [17], and hence, it is not shown in detail. Therefore, starting here from the state-space model, the transfer function relating the output voltage $(v_{\rm out})$ to input duty cycle (d) of the buck converter can be expressed as follows:

$$G_{dv}(s) = \frac{v_{\rm out}(s)}{d(s)} = \frac{V_{\rm in}(CR_C s + 1)}{s^2 LC\left(\frac{R_o + R_C}{R_O + R_L}\right) + S\left(R_C C + C\left(\frac{R_O R_L}{R_O + R_L}\right) + \frac{L}{R_O + R_L}\right) + 1}. \quad (1)$$

In (1), $V_{\rm in}$ is the input voltage, $R_{\rm O}$ is the load resistance, L is the inductance with dc resistance $R_{\rm L}$, and C is the output capacitance with equivalent series resistance $R_{\rm C}$. In Fig 1, the parasitic elements are included to improve the model accuracy and to demonstrate the importance of considering non-ideal components for system identification in applications such as power electronic converters. For instance, in the buck converter, the equivalent series resistor $R_{\rm C}$ cannot be ignored because it adds a zero to the transfer function (1), which has a negative impact on the dynamic behaviour of the converter [18]. In addition, its value may be used as a diagnostic indicator of capacitor aging [14]. In real-time applications, it is typical to use discrete analysis; hence, the digital equivalent transfer function is preferred [5], [14]. The transfer function parameters rely on the actual component values including the parasitic elements (such as R_L, R_C, and the conduction losses of the switch); therefore, a more accurate digital controller can be designed when the converter losses are considered. In this paper, a zero-order-hold mapping technique is applied to compute the equivalent discrete transfer function as follows:

$$G_{vd} = \frac{b_1 z^{-1} + b_2 z^{-2}}{1 + a_1 z^{-1} + a_2 z^{-2}}. \quad (2)$$

Here, the values of coefficients a and b are dependent on the Laplace transfer function coefficients defined in (1), and on the digital sampling time, T [2], [4].

B. ERLS for Parameter Estimation

In this paper, we apply the conventional ERLS scheme as a testbed for assessing the performance of the proposed KF

TABLE I
ERLS ADAPTIVE ALGORITHM

Step	Formula
Initialization	$P_0 = g * I$, and $\hat{\theta}_0 = 0$, where I is an $N \times N$ identity matrix, g is large number usually Do for k ≥ 1
1- Prediction error calculation	$\varepsilon_k = y_k - \varphi^T{}_k \hat{\theta}_{k-1}$
2-Calculate Kalman gain	$K_k = \frac{P_{k-1}\varphi_k}{(\lambda + \varphi^T{}_k P_{k-1}\varphi_k)}$
3-Update the parameter vector $\hat{\theta}$	$\hat{\theta}_k = \hat{\theta}_{k-1} + K_k \left(y_k - \varphi^T{}_k \hat{\theta}_{k-1}\right)$
4-Update the covariance matrix P	$P_k = \frac{1}{\lambda}\left[P_{k-1} - K_k \varphi^T{}_k\right]$

algorithm. To estimate the parameters in (2), the relation between the input and output signals can be rewritten as follows:

$$y_{\mathrm{k}} + a_1 y_{\mathrm{k}-1} + a_2 y_{\mathrm{k}-2} = b_1 u_{\mathrm{k}-1} + b_2 u_{\mathrm{k}-2} \tag{3}$$

where y_k and u_k denote the output voltage and the duty cycle control signal, respectively, at sampling instant k. For system identification purposes, the difference equation in (3) is rewritten in linear regression form

$$y_k = \varphi^T{}_k \theta_k. \tag{4}$$

By comparing (2) with (4), the unknown coefficients $[a_1\ a_2\ b_1\ b_2]$ are lumped in a vector $\theta_k \in R^N$, while the data vector φ_k (regression vector) contains the sampled input and output measurements. It is important to emphasize that minimizing the weighted sum of the quadratic error in (5) yields an accurate estimation of $\widehat{\theta}$ [2], [16]

$$E_{\min} = \sum_{k=1}^{n} \lambda^{n-k} \left(y_k - \varphi^T{}_k \hat{\theta}_k\right)^2 \tag{5}$$

where $(\lambda) \in [0, 1]$ is the forgetting factor, and n is the number of available samples to date. The estimated parameter vector $\hat{\theta}_k = [\hat{a}_1\ \hat{a}_2\ \hat{b}_1\ \hat{b}_2]$ is updated at every sampling instant through simple modification of $\hat{\theta}_{k-1}$. For conciseness, details of the algorithm are depicted in Table I [16]. In Table I, $P_k \in R^{N\times N}$ is the error covariance matrix, $K_k \in R^N$ is the adaptation gain vector or Kalman gain, and N is the number of parameters to be estimated. The initial choices of the system parameters $\hat{\theta}_0$ and covariance matrix P_0 are selected by the designer, and the role of experience and intuition is paramount [19].

C. KF Configured for Parameter Estimation

The KF is a mathematical method widely used to estimate unmeasured states using the measured input and output [20]. In this paper, the classical KF recursive algorithm is applied to estimate the set of unknown parameters θ_k instead of the states. This offers reduced convergence time, tracking performance, and estimation accuracy compared to other recursive algorithms [21]. As a result, one can consider a parameter variation model and a linear regression equation described by

$$\begin{aligned} y_k &= \varphi^T{}_k \theta_k + v_k \\ \theta_k &= \theta_{k-1} + w_k. \end{aligned} \tag{6}$$

TABLE II
KF CONFIGURED FOR PARAMETER ESTIMATION

Step	Formula
Initialization	$P(0) = g * I$, and $\hat{\theta}(0) = 0$, where I is an $N \times N$ identity matrix, g is large number, r is scalar > 0, Q is diag $[Q_{11}, Q_{22}, .., Q_{\mathrm{NN}}]$ Do for $k \geq 1$
'1-Kalman gain	$K_k = P^+_{k-1}\varphi^T_k \left[\varphi_k P^+_{k-1}\varphi^T_k + r_k\right]^{-1}$
2-Parameters estimate	$\hat{\theta}_k = \hat{\theta}_{k-1} + K_k \left[y_k - \varphi_k \hat{\theta}_{k-1}\right]$
3-Estimate dispersion update	$P_k = P^+_{k-1}(I - K_k \varphi_k)$
4-Covariance matrix project ahead	$P^+_k = P_k + \mathrm{Q}$

Here, the parameter changes are driven by random vector w_k with covariance matrix $Q \in R^{N\times N}$, and v_k is the observation noise with variance $r \in R$ [22].

Table II demonstrates the implementation sequence of the KF as a parameter estimator [22]. As shown in Table II, at the prediction step, the error covariance matrix is computed by the additional inclusion of a diagonal matrix Q to account for time-varying parameters. The size of the diagonal elements is conducive to the corresponding parameter variation in a random walk. Thus, the adaptation gain is adjusted for each parameter individually. This yields improved estimation accuracy for all elements in the vector θ with comparable convergence time and more flexibility in tuning. In contrast to the ERLS illustrated in Table I, a linear growth of the covariance matrix P is observed in the KF. As a result, the estimator may work for longer periods without any significant output perturbation and yet continues to exhibit operational responsiveness. This makes the KF approach an excellent option for real-time applications such as dc–dc converters where long periods of perturbation in the output voltage are highly undesirable.

D. KF Tuning

The tracking capability of the KF relies entirely on the value of Q, which has to be determined by the designer using offline tuning, until the desired filter output response is attained [19], [23]. However, this is a major challenge when using the KF for real-time state or parameter estimation. In this paper, an adaptive tuning method for determining Q is introduced. This approach was initially suggested for KF-based state estimation in [24]. However, here, a modified version of this tuning scheme is applied; each diagonal element in the matrix Q_{k} is calculated based on its related innovation term and Kalman gain. Therefore, individual parameters with different rates of variation can potentially be tracked more accurately. This is fundamentally different to many existing schemes. Referring to Table II, in step 2, the parameter variation can be estimated from

$$\widehat{w}_k = \widehat{\theta}_k - \widehat{\theta}_{k-1} = K_k \left[y_k - \varphi_k \widehat{\theta}_k\right]. \tag{7}$$

As a result, a different variance estimate is obtained for each element in the vector $\widehat{w}_k$ as follows:

$$\widehat{Q}_{ii}(k) = [\widehat{w}_i(k)]^2. \tag{8}$$

The deduced model error covariance in (9) is used to improve the tracking capability of the filter in the event of any sudden change in system parameters, such as abrupt load change in dc–dc converters

$$\widehat{Q}_k = diag[[\widehat{w}_1(k)]^2;\ [\widehat{w}_2(k)]^2;\ [\widehat{w}_3(k)]^2;\ [\widehat{w}_4(k)]^2]. \quad (9)$$

Using this matrix in step 4, each diagonal element in the error covariance matrix P will be updated according to the corresponding innovation term; hence, the components of parameter vector $\hat{\theta}_k$ will have a different variance estimate due to the assigned adaptation gain. This new tuning approach overcomes the difficulties faced in ERLS in estimating small parameters from noisy real-time data. Therefore, the estimation accuracy and the tracking performance can be improved significantly for all transfer function coefficients.

III. Simulation Results

In order to verify the performance of the proposed identification algorithm, a voltage-controlled synchronous dc–dc buck SMPC circuit is implemented in MATLAB/Simulink. The component values for the converter depicted in Fig. 1 are: $V_{\text{in}} = 10\,\text{V}$, $R_O = 5\,\Omega$, $L = 220\,\mu\text{H}$, $C = 330\,\mu\text{F}$, $R_C = 25\,\text{m}\Omega$, $R_L = 63\,\text{m}\Omega$, $R_{\text{DS(on)}} = 18\,\text{m}\Omega$, the switching frequency and sampling rate are 20 kHz, and the sensing gain is 0.5. The output voltage is regulated at 3.3 V using digital PID controller (10), designed based on the pole placement technique

$$G_C(z) = \frac{4.672 - 7.539\,z^{-1} + 3.184\,z^{-2}}{(1 - z^{-1})(1 + 0.374\,z^{-1})}. \quad (10)$$

In the early stages of the estimation process, no preliminary knowledge of the converter parameters is assumed. The same initial values of covariance matrix and parameter vector for both ERLS and KF are selected to be $P(0) = 10\,000\,I$, and $\hat{\theta}(0) = 0$. A 9-bit PRBS signal (a rich frequency excitation signal) is injected into the control signal to enhance the parameter estimation performance. To justify the identification results, the discrete transfer function of the average model in (11) is calculated in advance, at a sampling time of 50 μs. In line with many other sources of literature, convergence time and accuracy are considered to be the important metrics in evaluating the adaptive algorithm performance [2], [4]

$$G_{vd} = \frac{0.2262 + 0.1119\,z^{-2}}{1 - 1.913\,z^{-1} + 0.946\,z^{-2}}. \quad (11)$$

For the ERLS, the forgetting factor $\lambda = 0.95$ is carefully chosen to facilitate a compromise between estimator sensitivity and convergence speed. Unlike the preliminarily simulation results presented by the authors in [19], the modified tuning method in (9) is adopted in this paper to mitigate the disadvantages of using a trial-and-error procedure in the KF tuning and the measurement noise variance r is set to 0.095. Fig. 2 shows the parameter estimation results obtained using the ERLS identification algorithm and KF identification algorithm during the steady-state operation. As depicted in Fig. 2, both estimation algorithms rapidly identify the transfer function coefficients with final estimation values very close to the average model in (11). However, the KF estimation convergence to steady state is less than 0.5 ms, while the ERLS estimator takes around 1.5 ms to converge to the final values.

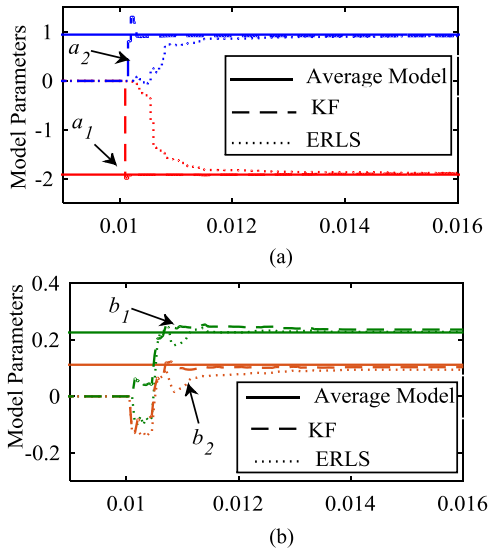

Fig. 2. Online parameter estimation results using ERLS and KF. (a) Denominator coefficients. (b) Numerator coefficients.

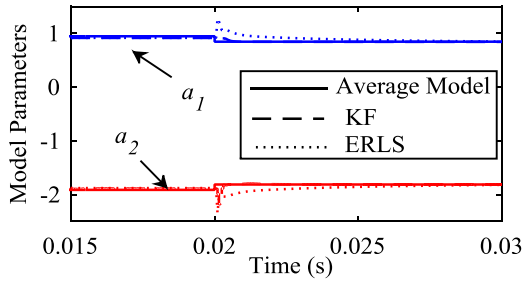

Fig. 3. Online parameters estimation during a step load change from 5 to 1 Ω at 0.02 s for ERLS and KF.

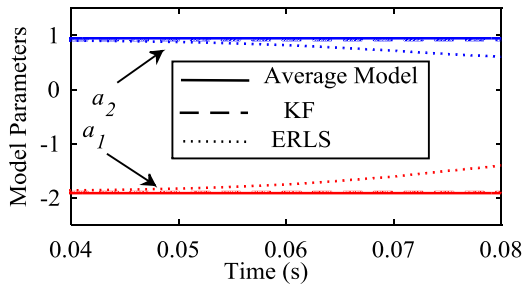

Fig. 4. Estimator win-up effect on ERLS and KF.

To further evaluate the performance of the propsed KF algorithm, a sudden and significant load change is applied at 0.02 s. The simulation results, illustrated in Fig. 3, indicate that after a sudden change in the load the KF identifies the transfer function denominator coefficients accurately with a convergence time less than 1 ms. In contrast, the ERLS estimation exhibits under/over shoot before it settles to the final values with a convergence time more than 5 ms. The stability of both identification algorithms is evaluated during the absence of the PRBS signal. The estimation results, shown in Fig. 4, demonstrate that the KF estimator has the ability to produce a smooth and stable

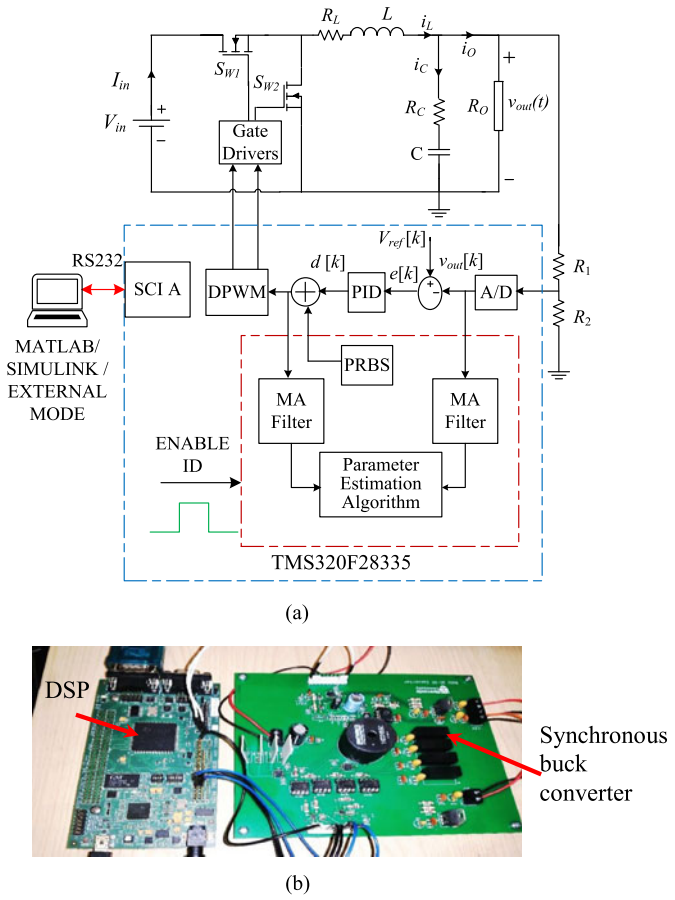

Fig. 5. Experimental setup of a synchronous buck converter for real-time parameter estimation. (a) Block diagram. (b) Overview of test board.

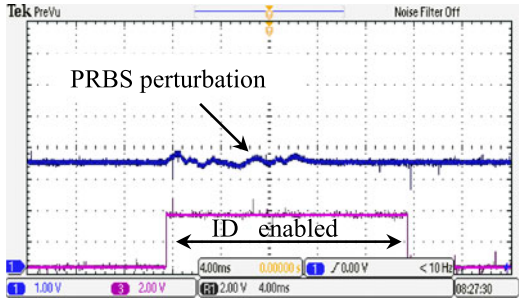

Fig. 6. Experimental output voltage during identification process with PRBS signal disabled after 10 ms.

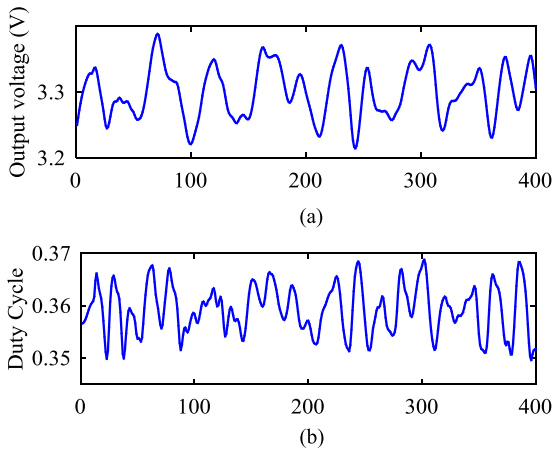

Fig. 7. Experimental filtered data sampled at 20 kHz. (a) Output voltage (zoom-in). (b) Duty cycle.

estimation with no effect of the estimator wind up. In contrast, the ERLS suffers from estimator the wind up phenomenon as the adaptation gain value increases over time and yields a clear offset in the final estimation value.

IV. Experimental Results

To validate the proposed algorithm, experimental verification is conducted on a 5-W synchronous buck converter. Fig. 5 shows the experimental setup for the proposed real-time parameter estimation algorithm. In order to compare the simulation and the experimental results, the converter parameters are selected to be the same as those outlined in Section III. In addition to the digital controller described in (10), the entire identification process including PRBS generation, filtering, and the adaptive algorithm is performed online on a Texas Instruments TMS320F28335 digital signal processor (DSP) platform to validate the proposed structure in real time. This is accomplished using the Embedded Coder Support package in MATLAB/Simulink to generate C code for all related blocks in the Simulink model and to run this model in "External Mode." This feature enables the user to tune and monitor the algorithm parameters in real time without stopping the application. The obtained real-time results are transferred to Simulink via a RS232 communication interface as shown in Fig. 5. To demonstrate the previously explained advantages of the KF over the ERLS algorithm, the identification process is enabled for 20 ms, while the PRBS signal is injected into the duty cycle for 10 ms only as depicted in Fig. 6. A small amplitude signal is selected for the excitation signal to keep the perturbation within 5% of the nominal output voltage during the identification procedure; it then reverts back to normal operation as shown in Fig. 6. Before real-time implementation, the proposed algorithm is tested offline to investigate the suitability of the data being used, the selected model structure, and the filter type. The logged output voltage and the control signal are both sampled at 20 kHz and exported to MATLAB. To accomplish a good estimation result, the measured output voltage and the control signal must be filtered before being applied to the estimation algorithm.

The filtering step is performed using a simple four tap moving average (MA) filter. These filtered signals are illustrated in Fig. 7. In the filtered output voltage [see Fig. 7(a)], the ripple content due to the excitation signal is approximately $\pm$ 2.5% with respect to the nominal dc output voltage. The achieved offline estimation results confirm that the presented model structure in (3) is suitable to describe the dynamics of the converter. Furthermore, the simple four-tap MA filter is sufficient to carry out the filtering task for a successful parameter estimation process. Due to space limitations, only real-time results are presented here as they are of primary importance.

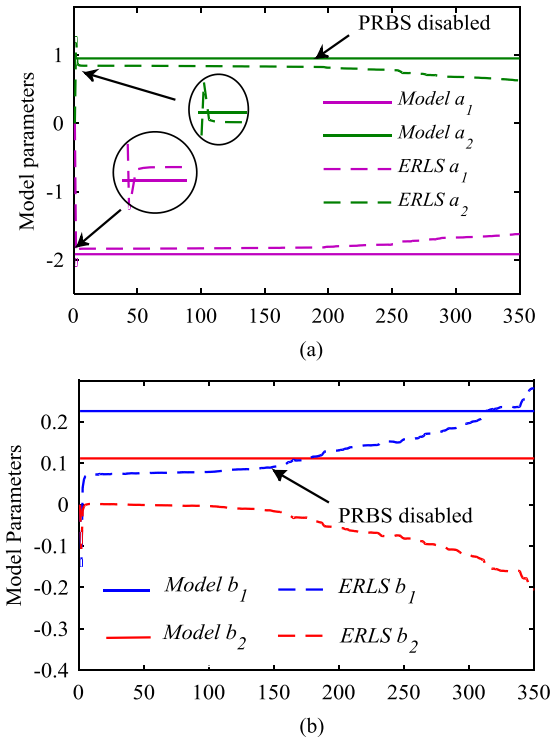

Fig. 8. Estimation results using ERLS with $\lambda = 0.95$. (a) Denominator coefficients. (b) Numerator coefficients.

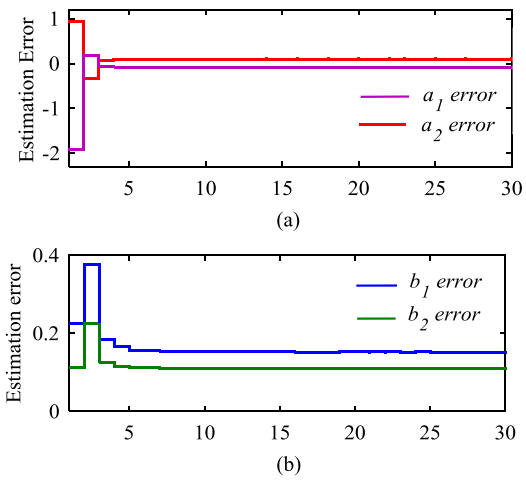

Fig. 9. Estimation error for ERLS during steady state operation. (a) Denominator coefficients. (b) Numerator coefficients.

A. ERLS Real-Time Results

Similar to the simulation procedure, the ERLS with forgetting factor $\lambda = 0.95$ is investigated. The online estimation results of the unknown parameters of the dc–dc model in (12) are illustrated in Fig. 8. As shown in Fig. 8, the ERLS requires around five samples (0.25 ms, at sampling time 50 μs) to converge to a steady-state value for the denominator coefficients (a_1, a_2) with accuracy range $\pm$ 7%, while the numerator taps take a longer time to converge (around 1 ms), and there is a clear offset in the final estimation. The limited accuracy of the ERLS estimator during the excitation period can be clearly demonstrated via the estimation error signal, as shown in Fig 9. Consequently, if the estimated coefficients are used for health monitoring purposes, as introduced in [14], inaccurate decisions may be taken in terms of predicting the health or age of the circuit components. In comparison with the simulation results presented earlier, the estimation accuracy of the ERLS estimator is highly affected by the measurement noise in the experimental implementation. To study the impact of the excitation signal on the estimation results, the PRBS signal is actively disabled after 10 ms, as shown in Fig. 6. Due to the scalar-forgetting factor used in ERLS, the estimated parameters start to deviate from steady state, which agrees with the simulation results in Fig. 4. This phenomenon is known as estimator wind-up, where the error covariance matrix grows exponentially and yields a high adaptation gain, as applied in the correction step [9]. Therefore, the ERLS is not a reliable estimator if a self-tuning controller is desired. Hence, in direct digital control design, such as the pole placement approach, the estimation results are fed to the controller directly and can potentially cause the system to be unstable since the values of (b_1, b_2) are not guaranteed to be accurate.

B. KF Real-Time Results

In this section, the proposed KF algorithm is evaluated. Similar to ERLS, the poles and zeroes parameters in (11) are compared with the average model parameters at a resistive load equal to 5 Ω. In Fig. 9, the parameters a_1 and a_2 converge to steady-state values in less than 0.15 ms, which is faster than the ERLS method with less over/undershoot and 0.3% estimation error. This confirms the simulation result depicted in Fig. 2. In comparison with ERLS, the parameters b_1 and b_2 are estimated within a similar period of time, but with enhanced accuracy. Importantly, the execution time of the proposed KF, measured in real time using Code Composer Studio, is only 3 μs longer than the ERLS. Similarly, to ERLS, the stability of the KF is examined when the PRBS signal is disabled. As shown in Fig. 10, KF has the ability to produce a smooth and stable estimation with no effect of the estimator wind up. Therefore, the obtained results can provide a stable self-tuning compensator since the zero coefficients do not fluctuate and stay very close to the pre-calculated ones. In addition, the observed prediction error illustrated in Figs. 10 and 11 confirms the advantages of the KF over the ERLS in terms of accuracy and improved convergence speed for transfer function estimation. The results obtained for both investigated algorithms are summarized in Table III, which demonstrates that the KF outperforms ERLS in terms of accuracy and convergence time. Only a very small amount of additional execution time is required, due to the tuning step introduced in (9). In Table III, the achieved real-time results show that the KF approach outperforms the classical ERLS in terms of accuracy of all transfer function coefficients, as well as the minimal convergence time required to reach the steady state. Importantly, in comparison to similar tests introduced in [2] and [14], in this paper, all system identification steps, including filtering and the adaptive algorithm implementation, are performed online without interrupting the normal system operation.

Here, the sampling frequency is set similar to the converter switching frequency to take one sample of the output voltage

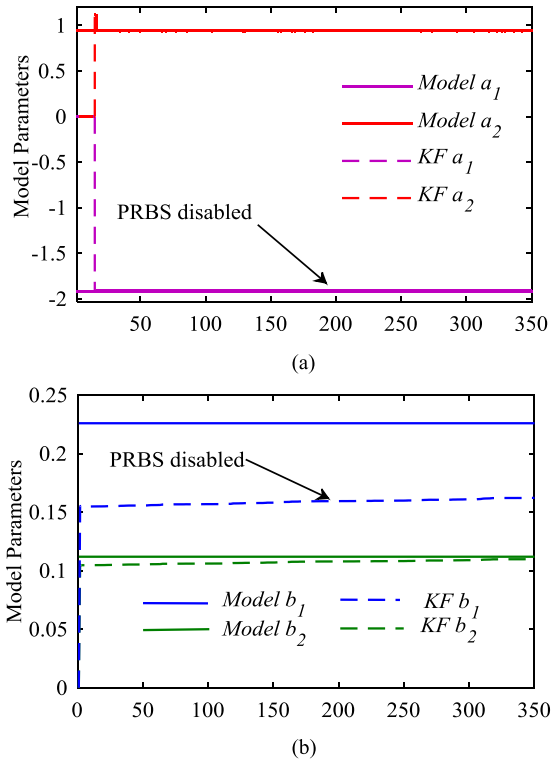

Fig. 10. Estimation results using KF. (a) Denominator coefficients. (b) Numerator coefficients.

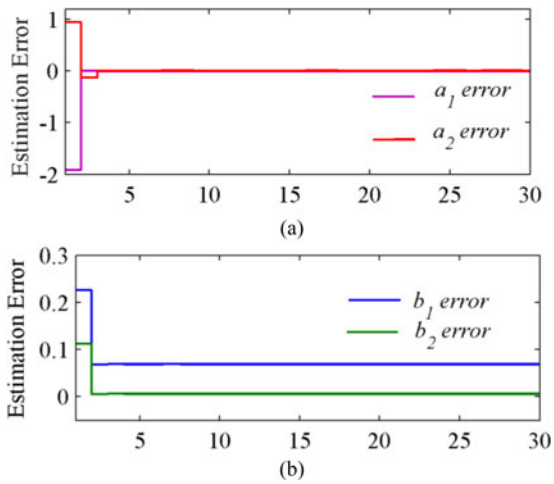

Fig. 11. Estimation error for KF during steady-state operation. (a) Denominator coefficients. (b) Numerator coefficients.

TABLE III
STEADY-STATE PARAMETER ESTIMATION COMPARISON BETWEEN ERLS AND KF

Parameter	KF	ERLS	MODEL
$a1$	−1.922	−1.822	−1.913
$a2$	0.946	0.842	0.946
$b1$	0.161	0.087	0.2259
$b2$	0.0991	−0.00573	0.1119
Convergence time	0.15 ms	0.25 ms	
Computational time per iteration	37 µs	33 µs	

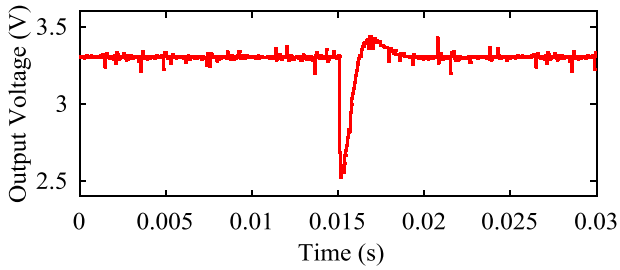

Fig. 12. Output voltage recorded on the DSP during a step load change from 5 to 1 Ω at 0.015 s.

and the control signal every switching period, while in [14], a slow sampling rate is selected, which leads to a very slow convergence time. Furthermore, the impact of the excitation signal on the estimator behavior is examined here and confirms that the KF approach does not require long perturbation periods to achieve accurate and robust estimation results. Therefore, if a similar mapping method to that presented in [14] is applied on KF estimation, the values of the converter components such as *L, C* can be easily and accurately extracted online. Even though low computational effort is required in the estimation algorithm proposed in [2], the same shortcoming of the ERLS is observed where the numerator parameters are highly effected by measurement noise hence the final estimation cannot be used for health monitoring or self-tuning controller design.

C. Parameter Estimation During Abrupt Load Change

In SMPC, it is well recognized that the mode of operation can potentially be diverted from CCM to discontinuous conducting mode if a wide load variation is applied; as a result, loop stability margins are decreased and the converter may exhibit instability upon the mode transition [25]. Traditionally, this phenomenon is treated by designing a conservative controller (effectively a worst-case design) to cope with any abrupt changes and ensure the system stability.

Therefore, it is a great benefit if the load value is estimated and the controller is tuned to meet the desired bandwidth and stability margins. For this reason, a wide and abrupt load change is applied to further investigate the performance of the proposed self-tuned KF. Fig. 12 shows the dynamic response of the output voltage when the load is changed from 5 to 1 Ω at 0.015 s. As previously confirmed, the KF provide excellent estimation performance without any perturbation in the observed data. This can be seen clearly in the recorded output voltage in Fig. 12, where no excitation signal is injected. This scenario is deliberately applied, because in the case of ERLS, the estimated parameters deviate immediately once the PRBS is disabled, so if the load changes after this instant, the ERLS is unable to detect the new variation and another perturbation period is required to perform the estimation process. Therefore, a PRBS signal is injected before the step change applied to investigate the performance of ERLS during load variation. On the other hand, the KF estimator stays alert to the situation for a longer period; hence, no perturbation is required to detect the load change. Fig. 13(a) shows the KF estimation results, with the transfer

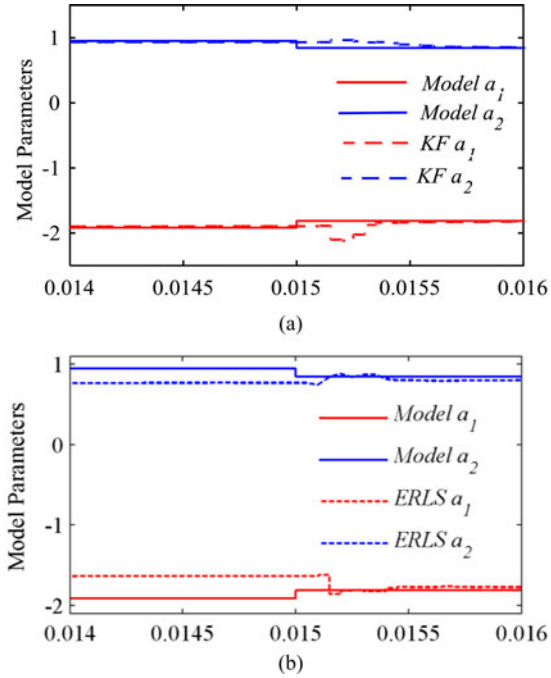

Fig. 13. Real-time parameters estimation during a step load change from 5 to 1 Ω at 0.015 s. (a) KF. (b) ERLS.

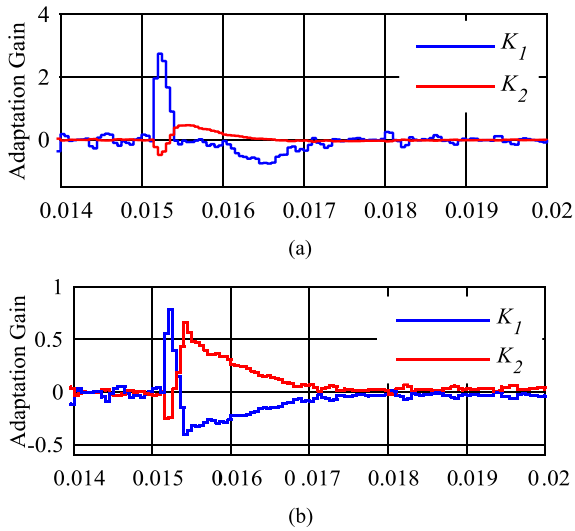

Fig. 14. Kalman gains. (a) KF. (b) ERLS.

function poles accurately estimated before and after the load change with convergence time less than 1 ms. In contrast, the ERLS estimation has a clear offset during steady state, which improves after the load change as illustrated in Fig. 13(b). This behavior confirms that the ERLS estimator requires a large perturbation signal to provide accurate and reliable estimation. It is worth noting that, the numerator parameters are not illustrated here due to the small effect of the load change that can be ignored according to the computed transfer function

$$G_{vd} = \frac{0.2243\ z^{-1} + 0.1062\ z^{-2}}{1 - 1.814\ z^{-1} + 0.8437\ z^{-2}}. \tag{12}$$

To demonstrate the advantages of using the proposed tuning method, the related adaptation gains of a_1 and a_2 are recorded in steady state and during the load change as illustrated in Fig. 14(a). As stated in (11), each element in the matrix Q is tuned accordingly to the contribution of the related parameter vector component in the estimator output $(\varphi_k \hat{\theta}_k)$. Therefore, the assigned Kalman gain elements for K_1 for a_1, and K_2 for a_2, vary with different rates in the correction step. This yields improved overall tracking performance to the newly applied load. This variation is confirmed by referring to (12) and (13), where parameter a_1 decreases by 5.5% and a_2 simultaneously decreases by 1% when the load abruptly reduces from 5 to 1 Ω. Therefore, the impact of load change varies between one coefficient and another in the discrete transfer function. In contrast, the ERLS algorithm react to the load change by applying similar magnitude with different directions for both a_1 and a_2 in the correction step, due to the single forgetting factor scheme as shown in Fig. 14(b). Thus, the KF approach is considered to be the ideal candidate in this case to provide reliable estimation for time-varying parameters; such as load change which is a common scenario in power converter applications.

V. Conclusion

This paper presents a new real-time parameter estimation technique for dc–dc converter systems, based on a self-tuned KF approach. The proposed technique has the potential for use in real-time system identification and adaptive control systems for power electronic applications, such as switch mode power supplies. The mathematical description of the proposed algorithm is presented, and the algorithm is fully validated using a digitally controlled buck power converter. In this paper, unlike a significant proportion of existing literature, the entire system identification and closed-loop control process is seamlessly implemented in real-time hardware, without any remote intermediate post processing analysis. Experimental results show that the proposed KF provides accurate and fast estimation of the discrete transfer function. The performance of the KF is also tested without a perturbation signal, and the results obtained prove that the covariance matrix update scheme keeps the estimator stable and responsive for longer periods of time. Furthermore, and important from a practical perspective, the effect of estimator wind up is reduced. Additionally, a new state-of-the-art tuning method for the process covariance matrix has been introduced to optimize convergence speed and allow the estimator to track time-varying parameters. The advantage of this has been successfully validated via an abrupt step change in load.

References

[1] H. Renaudineau, J. P. Martin, M. B. Nahid, and S. Pierfederici, "DC-DC converters dynamic modeling with state observer-based parameter estimation," *IEEE Trans. Power Electron.*, vol. 30, no. 6, pp. 3356–3363, Jun. 2015.

[2] M. Algreer, M. Armstrong, and D. Giaouris, "Active online system identification of switch mode DC-DC power converter based on efficient recursive DCD-IIR adaptive filter," *IEEE Trans. Power Electron.*, vol. 27, no. 11, pp. 4425–4435, Jun. 2012.

[3] R.-J. Wai, Y.-F. Lin, and Y.-K. Liu, "Design of adaptive fuzzy-neural-network control for single-stage boost inverter," *IEEE Trans. Power Electron.*, vol. 30, no. 12, pp. 7282–7298, Dec. 2015.
[4] G. E. Pitel and P. T. Krein, "Real-time system identification for load monitoring and transient handling of DC–DC supplies," in *Proc. IEEE Power Electron. Spec. Conf.*, 2008, pp. 3807–3813.
[5] M. M. Peretz and S. Ben-Yaakov, "Time-domain identification of pulse-width modulated converters," *IET Power Electron.*, vol. 5, pp. 166–172, 2012.
[6] M. Bhardwaj, S. Choudhury, R. Poley, and B. Akin, "Online frequency response Analysis: A powerful Plug-in Tool for compensation design and health assessment of digitally controlled power converters," *IEEE Trans. Ind. Appl.*, vol. 52, no. 3, pp. 2426–2435, May/Jun. 2016.
[7] L. Jun-Yan, Y. Chun-Hung, and T. Chien-Hung, "Correlation-based system identification of digitally controlled SMPS," in *Proc. IEEE 9th Int. Conf. Power Electron. Drive Syst.*, 2011, pp. 1149–1152.
[8] A. Barkely and E. Santi, "Improved online identification of a DC–DC converter and its control loop gain using cross- correlation methods," *IEEE Trans. Power Electron.*, vol. 24, no. 8, pp. 2021–2031, Aug. 2009.
[9] L. Ljung, *System Identification: Theory for the User*. 2nd ed. Upper Saddle River, NJ, USA: Prentice-Hall, 1999.
[10] B. Johansson and M. Lenells, "Possibilities of obtaining small-signal models of dc–dc power converters by means of system identification," in *Proc. Telecommun. Energy Conf.*, 2000, pp. 65–75.
[11] M. Shirazi, J. Morroni, A. Dolgov, R. Zane, and D. Maksimovic, "Integration of frequency response measurement capabilities in digital controllers for DC–DC converters," *IEEE Trans. Power Electron.*, vol. 23, no. 5, pp. 2524–2535, Sep. 2008.
[12] J. Castello and J. M. Espi, "DSP implementation for measuring the loop gain frequency response of digitally controlled power converters," *IEEE Trans. Power Electron.*, vol. 27, no. 9, pp. 4113–4121, Sep. 2012.
[13] F. Alonge, F. D'Ippolito, F. M. Raimondi, and S. Tumminaro, "Nonlinear modelling of DC/DC converters using the Hammerstein's approach," *IEEE Trans. Power Electron.*, vol. 22, no. 4, pp. 1210–1221, Jul. 2007.
[14] B. X. Li and K. S. Low, "Low sampling rate online parameters monitoring of DC-DC converters for predictive-maintenance using biogeography-based optimization," *IEEE Trans. Power Electron.*, vol. 31, no. 4, pp. 2870–2879, Apr. 2016.
[15] M. Algreer, M. Armstrong, and D. Giaouris, "System identification of PWM DC–DC converters during abrupt load changes," in *Proc. 35th Annu. Conf. IEEE Ind. Electron.*, 2009, pp. 1788–1793.
[16] A. Vahidi, A. Stefanopoulou, and H. Peng, "Recursive least squares with forgetting for online estimation of vehicle mass and road grade: Theory and experiments," *Veh. Syst. Dyn.*, vol. 43, pp. 31–55, 2005.
[17] L. Corradini, D. Maksimovic, P. Mattavelli, and R. Zane, "Continuous-time averaged modeling of DC-DC converters," in *Digital Control of High-Frequency Switched-Mode Power Converters*. Hoboken, NJ, USA: Wiley-IEEE Press, 2015, pp. 1–360.
[18] R. Redl and J. Sun, "Ripple-based control of switching regulators: An overview," *IEEE Trans. Power Electron.*, vol. 24, no. 12, pp. 2669–2680, Dec. 2009.
[19] M. Ahmeid, M. Armstrong, S. Gadoue, and P. Missailidis, "Parameter estimation of a DC-DC converter using a Kalman filter approach," in *Proc. 17th IET Int. Conf. Power Electron., Mach. Drives*, 2014, pp. 1–6.
[20] M. A. Eleffendi and C. M. Johnson, "Application of Kalman filter to estimate junction temperature in IGBT power modules," *IEEE Trans. Power Electron.*, vol. 31, no. 2, pp. 1576–1587, Feb. 2016.
[21] O. Rosen and A. Medvedev, "Efficient parallel implementation of a Kalman filter for single output systems on multicore computational platforms," in *Proc. 2011 50th IEEE Conf. Decision Control Eur. Control Conf.*, 2011, pp. 3178–3183.
[22] L. Cao and H. M. Schwartz, "Analysis of the Kalman filter based estimation algorithm: An orthogonal decomposition approach," *Automatica*, vol. 40, pp. 5–19, 2004.
[23] G. Welch and G. Bishop, "An introduction to the Kalman filter," Dept. Comput. Sci., Univ. North Carolina, Chapel Hill, NC, USA, unpublished manuscript, 2006.
[24] J. A. R. Macias and A. Gomez-Exposito, "Self-tuning of Kalman filters for digital protection applications," in *Proc. 2005 IEEE Russia Power Tech*, 2005, pp. 1–4.
[25] J. Morroni, L. Corradini, R. Zane, and D. Maksimovic, "Adaptive tuning of switched-mode power supplies operating in discontinuous and continuous conduction modes," *IEEE Trans. Power Electron.*, vol. 24, no. 11, pp. 2603–2611, Nov. 2009.

Mohamed Ahmeid received the B.Sc. degree in automatic control from the College of Electronic Technology, Bani Walid, Libya, in 2003, and the M.Sc. degree in automation and control from Newcastle University, Newcastle Upon Tyne, U.K., in 2010, where he is currently working toward the Ph.D. degree in electrical and electronic engineering.

From 2005 to 2008 and from 2010 to 2012, he was a Senior Commissioning Engineer with the General Electricity Company of Libya. His research interests include system identification real-time digital control of power electronic converters, adaptive filtering, and autonomous ground vehicle control using artificial intelligent methods.

Matthew Armstrong received the M.Eng. and Ph.D. degrees from Newcastle University, Newcastle Upon Tyne, U.K., in 1998 and 2007, respectively.

He is currently a Senior Lecturer in control of electrical power at Newcastle University. He has more than 18 years' experience in the fields of electric drives, grid-connected renewable energy systems, hardware-in-the-loop emulation, and Li-ion battery characterization and fault detection. His current research interests include real-time parameter estimation, system identification, and advanced adaptive control of power electronic systems.

Shady Gadoue received the B.Sc. and M.Sc. degrees from Alexandria University, Alexandria, Egypt, in 2000 and 2003, respectively, and the Ph.D. degree from Newcastle University, Newcastle upon Tyne, U.K., in 2009, all in electrical engineering.

From 2009 to 2011, he was an Assistant Professor with the Department of Electrical Engineering, Alexandria University, where he was an Assistant Lecturer from 2000 to 2005. In 2011, he joined the Electrical Power Research Group, Newcastle University, as a Lecturer in Control Systems. Since March 2016, he has been a visiting member of academic staff with the Control and Power Research Group, Imperial College London, London, U.K. His main research interests include control, state and parameter identification, and optimization algorithms applied to energy conversion, and power electronic systems.

Maher Al-Greer received the B.Sc. degree in electrical engineering and the M.Sc. degree in computer engineering from the University of Mosul, Mosul, Iraq, in 1999 and 2005, respectively, and the Ph.D. degree in electrical and electronic engineering from Newcastle University, Newcastle upon Tyne, U.K., in 2012.

From 2001 to 2015, he was with the University of Mosul as a Demonstrator, Assistance Lecturer, and Lecturer. He is currently a Postdoctoral Research Associate at Newcastle University, working on Innovate UK project. His research interests include signal-processing techniques for power electronics systems, system identification, digital power control, adaptive control, diagnosis and monitoring of power converters, power semiconductor devices, embedded control design, fuzzy logic, and motor drive control.

Petros Missailidis received the B.S. degree in mechanical engineering from Aristotelian University of Thessaloniki, Thessaloniki, Greece, in 1986, the M.S. degree in mechanical engineering from the University of Buffalo, Buffalo, NY, USA, in 1990, the M.S. degree in electrical and electronic engineering and biomedical engineering from Rensselaer Polytechnic Institute, Troy, NY, in 1993, the M.S. degree in mechanical engineering from the same institute in 1995, and the Ph.D. degree in mechanical engineering from Rensselaer Polytechnic Institute, Troy, in 2000.

He was with ComHouse Wireless Inc., M/A-COM Inc., General Electric Schenectady NY, Erie County Medical Centre, Buffalo, and the University of Toronto. He is currently with the School of Electrical and Electronics Engineering, Newcastle University, Newcastle upon Tyne, U.K., where he is involved in conducting research in the areas of system identification, nonlinear control, and control of electric drives.